
Article:
Idrees, S.M., Waite, S.L., Granados Aparici, S. et al. (2024) Nicotine exposure is associated with targeted impairments in primordial follicle phenotype in cultured neonatal mouse ovaries. Ecotoxicology and Environmental Safety, 288. 117302. ISSN: 0147-6513

https://doi.org/10.1016/j.ecoenv.2024.117302

Ecotoxicology and Environmental Safety 288 (2024) 117302

Contents lists available at ScienceDirect

Ecotoxicology and Environmental Safety

journal homepage: www.elsevier.com/locate/ecoenv

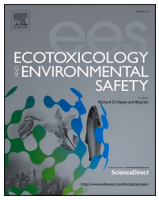

Nicotine exposure is associated with targeted impairments in primordial follicle phenotype in cultured neonatal mouse ovaries

Sara M. Idrees, Sarah L. Waite, Sofia Granados Aparici [1,2], Mark A. Fenwick [*]

Division of Clinical Medicine, School of Medicine and Population Health, University of Sheffield, Sheffield S10 2SF, UK

ARTICLE INFO

Edited by Richard Handy

Keywords:
Nicotine
Ovary
Ovarian reserve
Primordial follicle
Oocyte
Granulosa cells

ABSTRACT

The ovarian reserve consists of a limited supply of primordial follicles (PFs), each containing an oocyte surrounded by a layer of granulosa cells (GCs). PFs are relatively quiescent and must remain viable for a long period, thereby making them susceptible to environmental and lifestyle influences. Given the widespread prevalence of e-cigarette use, this study aimed to investigate the effects of nicotine and its metabolite cotinine in a mouse model and to elucidate the mechanisms by which nicotine influences the ovarian reserve. Neonatal ovaries were cultured for 7-days in nicotine or cotinine reflective of concentrations in plasma of e-cigarette users. From histological evaluation, nicotine or cotinine had no impact on the number of PFs or early growing follicles; however, the medium (15 ng/ml) and high (45 ng/ml) concentrations of nicotine (but not cotinine) caused a small reduction in oocyte and GC size within PFs relative to controls (0 ng/ml; both $P<0.01$). These morphological effects were not associated with changes in immunofluorescent markers of apoptosis (active caspase-3) or proliferation (Pcna), but were associated with increased gH2AX in PF oocytes, indicative of DNA damage and repair. RNA-sequencing of cultured ovaries exposed to nicotine (45 ng/ml) relative to control (0 ng/ml), revealed a suite of differentially expressed candidates, as well as numerous gene ontology biological processes associated with increased DNA damage, metabolism, respiration and immune function, alongside suppression of meiosis, cell adhesion, differentiation and morphogenesis. Findings from this study indicate that direct nicotine exposure has a limited effect on the quantity of PFs, but importantly highlights a range of processes that could impinge on the quality of the ovarian reserve.

1. Introduction

The ovarian reserve is a term that refers to the population of small, non-growing and non-renewable, primordial-staged follicles in the ovary (Findlay et al., 2015). Each primordial follicle (PF) consists of a meiotically-arrested oocyte enveloped by a single layer of squamous granulosa cells. In humans, PFs form in the fetal ovary during mid-gestation, whereas the equivalent process occurs in mice during the first few days after birth (Tingen et al., 2009). To maintain reproductive function over time, PFs must remain viable in this arrested state until recruited for development. However, long-term preservation predisposes them to the ageing process as well as harmful influences from the environment. Thus, lifestyle choices of the individual can significantly impact the quality and quantity of the ovarian reserve.

It has long been established from epidemiological studies that women prenatally exposed to cigarette smoke have reduced fecundity (Weinberg et al., 1989). Furthermore, women who smoke, as well as their female offspring, tend to enter menopause early, suggesting a possible effect on the ovarian reserve (Di Prospero et al., 2004, Harlow and Signorello, 2000, Oboni et al., 2016). Indeed, studies in rodents have shown that direct exposure to cigarette smoke leads to a significant reduction in the number of PFs (Li et al., 2020, Li et al., 2022, Sobinoff et al., 2013, Tuttle et al., 2009). In addition, exposure to products of cigarette combustion such as benzo(a)pyrenes and polycylic aromatic hydrocarbons, also cause PF loss, which occurs through apoptosis-initiated or autophagy-related mechanisms (Furlong et al., 2015, Gannon et al., 2012, Jurisicova et al., 2007, Li et al., 2020, Tuttle et al., 2009).

* Correspondence to: Reproductive and Developmental Medicine, Level 4 The Jessop Wing, Division of Clinical Medicine, School of Medicine and Population Health, Faculty of Health, University of Sheffield, Sheffield S10 2SF, UK.
E-mail address: m.a.fenwick@sheffield.ac.uk (M.A. Fenwick).
[1] Cancer CIBER (CIBERONC), Madrid, Spain
[2] Pathology Department, Medical School, University of Valencia-INCLIVA, Valencia, Spain

https://doi.org/10.1016/j.ecoenv.2024.117302
Received 18 July 2024; Received in revised form 29 October 2024; Accepted 5 November 2024

Chemicals from cigarette smoke (of which there are >4000) have been extensively studied in a range of biological systems due to their known carcinogenic properties and general negative effects on health. This has prompted a recent shift in consumer demand for less harmful alternatives such as e-cigarettes (Farsalinos et al., 2015, Lindson et al., 2024). Recent meta-analyses and surveys indicate a worldwide increase in e-cigarette usage, particularly among teenagers and young adults (Hammond et al., 2020, Tehrani et al., 2022). Although it is generally accepted that e-cigarettes are less harmful than tobacco cigarettes, the effects of chronic ingestion of nicotine and metabolised products, on reproductive health are still not well understood.

In mouse models, nicotine exposure around the perinatal period causes a delay in PF formation, often accompanied by elevated markers of oxidative stress, DNA damage and autophagy-related genes (Liu et al., 2020, Liu et al., 2021, Wang et al., 2018). Similar findings have been reported in human fetal ovaries exposed to nicotine *in vitro*, leading to a large reduction in germ cell number and increased evidence of apoptosis (Cheng et al., 2018). Limited studies have also reported a nicotine-induced reduction in PF number; however, the molecular mechanisms accounting for this loss are unclear, since markers for proliferation or apoptosis in the granulosa cells or oocytes of PFs exposed to nicotine were unchanged relative to controls (Faghani et al., 2022, Sezer et al., 2020). Therefore, the extent to which nicotine affects the ovarian reserve and the mechanisms by which it does so remain unclear.

Nicotine exerts its effects by binding and activating nicotinic acetylcholine receptors (nAChRs). Mature nAChRs are composed of specific nAChR sub-types arranged to form a functional pentameric receptor (Albuquerque et al., 2009). It is now recognized that these receptors are commonly expressed in a wide range of cell types outside of the nervous system including granulosa cells and oocytes of primordial follicles (Cheng et al., 2018, Liu et al., 2020, Mourikes et al., 2024, Wang et al., 2018). Approximately 70 %-80 % of nicotine in humans is metabolised by the liver enzyme Cytochrome P450 2A6 (CYP2A6) to cotinine (Dempsey et al., 2002). In humans, cotinine has been detected in granulosa cells and follicular fluid of mature follicles (Zenzes et al., 1997, Zenzes and Reed, 1998), indicating that cotinine can access the ovary and potentially exert effects locally. Cotinine has the ability to bind and activate nAChRs (Dwoskin et al., 1999); however, whether cotinine has any effect on the ovarian reserve is currently unknown.

Although nicotine can have a profound impact on the formation of the ovarian reserve, it is not clear whether nicotine and cotinine can directly affect the quality and quantity of PFs once they are formed. To address this question, this study utilised postnatal day 4 (PND4) mouse ovaries as an *in vitro* model to investigate the direct effects of these compounds on PFs and to elucidate the mechanisms of action through transcriptomic analysis using RNA-sequencing.

2. Materials and methods

2.1. Animals and tissues

Wild-type C57BL/6 mice were used in accordance with UK Home Office regulations and adherence to the Animals (Scientific Procedures) Act (1986). Animals were killed using Schedule 1 procedures by a trained and registered practitioner at the University of Sheffield. For all culture experiments, postnatal day 4 (PND4) mice were used due to the small size of the ovaries and the preponderance of primordial follicles (Fenwick et al., 2011). Reproductive tracts were dissected from mice and placed in warmed Liebovitz L-15 medium (Gibco, ThermoFisher) containing 1 % (w/v) bovine serum albumin (BSA; Sigma-Aldrich) prior to further microdissection. For qPCR analysis of nAChR transcripts, ovaries (n) were retrieved from juvenile mice under a dissection microscope (PND4, n=6; PND8, n=5; PND16, n=6) and immediately frozen in liquid nitrogen and stored at −80°C prior to RNA isolation.

2.2. RNA isolation, cDNA and qPCR

Total RNA was isolated from ovaries of juvenile mice or ovaries cultured in different concentrations of nicotine using Qiagen RNeasy micro kits, which includes a DNase digestion step (Qiagen, Crawley, UK). RNA concentration and integrity were measured using an Agilent 2100 Bioanalyser (Agilent Technologies Inc., CA, USA) and 50 ng of each sample was converted to cDNA using SuperScript IV First Strand Synthesis kit (Invitrogen, ThermoFisher, Cheshire, UK). One μl of cDNA was added to a reaction of KAPA SYBR Fast (Sigma-Aldrich, Dorset, UK), 400 nM gene specific primers (Suppl. Table 1) and nuclease free water in duplicate in a 384-well plate. Reaction conditions were set to 40 cycles of denaturation (95°C), annealing (58–60°C) and extension (72°C) as per reagent guidelines (KAPA) in a 7900HT Fast Real-Time PCR machine (Applied Biosystems). Technical replicates, amplicon-specific melt curves and no-template (negative) control samples were evaluated for quality control purposes. Relative fold changes between groups were determined using the $2^{-\Delta\Delta CT}$ method (Livak and Schmittgen, 2001) using *Hprt1* (Suppl. Table 1) as the internal reference for the uncultured ovaries or a commercially designed primer pair targeting *Atp5b* (PrimerDesign, Southampton, UK) for the cultured ovary samples.

2.3. Neonatal ovary culture

PND4 ovaries were cleanly micro-dissected and positioned on permeable membrane inserts in 24 mm Transwell® plates (Corning, ThermoFisher) beneath the meniscus of the culture medium (3 per well). Culture medium consisted of Waymouth medium 752/1 (Life Technologies) supplemented with 10 % (v/v) fetal bovine serum (ThermoFisher Scientific), 0.23 mM pyruvic acid (Sigma), 10 μg/ml streptomycin sulphate (Sigma), 75 μg/ml penicillin G (Sigma) and 0.3 mg/ml BSA as used previously (Eppig and O'brien, 1996, Granados-Aparici et al., 2019). Ovaries were exposed to racemic nicotine (N0267; Sigma) or cotinine (C5923; Sigma) using concentrations consistent with published plasma levels from e-cigarette users (Dawkins and Corcoran, 2014, Farsalinos et al., 2015, Flouris et al., 2013, Vansickel and Eissenberg, 2013). Specifically, 5 ng/ml was considered as a low concentration of nicotine, 15 ng/ml was considered medium concentration and 45 ng/ml was considered a high concentration. For cotinine, 12 ng/ml, 60 ng/ml and 300 ng/ml were considered as low, medium and high concentrations, respectively. No nicotine or cotinine was added to control groups. All ovaries were maintained for 7 days at 37°C with 5 % CO2 with full media changes every second day. At the end of culture, ovaries were rinsed in PBS before immersing for 2 h in 10 % neutral buffered formalin (Sigma) for fixation or immediately frozen in liquid nitrogen and stored at −80°C for downstream RNA analyses.

2.4. Immunostaining and imaging

Fixed ovaries were processed and embedded in paraffin, serially sectioned (5 μm) and mounted on positively charged slides (Superfrost Plus®, ThermoFisher). Approximately 15–20 sections were obtained from each cultured ovary and a single section near the centre of the ovary was selected for staining with each of the antibodies listed below. The number of ovaries cultured and processed for immunostaining totalled 6, 7, 7, 7 for 0, 5, 15, 45 ng/ml nicotine groups, respectively and 9, 9, 9, 8 for 0, 12, 60, 300 ng/ml cotinine groups, respectively. Sections were dewaxed, rehydrated through decreasing concentrations of ethanol prior to heating for 4×5 mins in 0.01 M citrate buffer (pH 6.0) for antigen retrieval. After washing in PBS, CAS-Block® universal blocking solution (ThermoFisher) was applied to sections for 15 minutes at room temperature to reduce non-specific binding. Specific antibodies against Smad2/3 (0.25 μg/ml, 133098, Santa Cruz Biotechnology, TX, USA), Ddx4 (4 μg/ml, ab13840, Abcam, Cambridge, UK), active caspase-3 (1:200 dilution, 9664, Cell Signalling Technology, Leiden, The Netherlands), Pcna (0.4 μg/ml, PC10, Santa Cruz Biotechnology), and

gamma H2ax (1 μg/ml, NB100–384, Novus Biologicals, CO, USA) were diluted in CAS solution and applied to sections overnight at 4°C in a humidified chamber in accordance with previous studies (Fenwick and Hurst, 2002, Hardy et al., 2018). Within each staining protocol, a negative control mouse IgG (I-200; Vector) or rabbit IgG (I-1000; Vector) was added to a section at the equivalent concentration of the specific primary antibody used. For double labelling, both primary antibodies or control IgGs were incubated together. Sections were washed 3×10 mins in PBS and incubated with secondary antibodies at 1:400 dilution (either donkey anti-mouse or rabbit AlexaFluor® 555, A32790/A32773) or donkey anti-rabbit AlexaFluor® 488, A21206; Invitrogen) for 45 minutes. Sections were mounted with aqueous anti-fade (Prolong® Gold; Invitrogen) with DAPI and coverslipped. Images were obtained with a Leica inverted SP5 confocal laser-scanning microscope (Leica Microsystems, Wetzlar, Germany) using an oil-immersion 40x objective. The tile scan function allowed images across each section to be digitally stitched together to create a high-resolution composite. Laser power and gain/offset settings were kept consistent within each immunofluorescence experiment where the objective was to quantify staining intensity.

2.5. Follicle classification, morphology measurements and quantification of staining

For morphological analyses and quantification of staining, a single mid-section was analysed from an ovary from each of the nicotine treated and cotinine treated groups. Confocal images were imported into ImageJ software (https://imagej.nih.gov/ij/) and follicles were selected for measurement if a clearly identifiable oocyte nucleus was evident (using Ddx4 as a cytoplasmic oocyte marker). Follicles were classified on the basis of the number of GCs surrounding the oocyte, as facilitated by the GC-specific stain, Smad2/3 (Granados-Aparici et al., 2019, Hardy et al., 2018). Primordial follicles consisted of 1–3 flat GCs surrounding the oocyte, transitional follicles contained 4–7 GCs that were either all flat, or a mixture of flat and cuboidal morphology. Follicles with >7 GCs surrounding the oocyte, regardless of morphology or number of GC layers were considered to be growing (Granados-Aparici et al., 2019). For each classified follicle, oocyte area and follicle area were manually determined using the measure function in ImageJ by tracing around the oocyte and basement membrane, respectively. GC area was derived as the difference between the two. To quantify Pcna expression, images were converted to an 8-bit RGB stack file and a consistent threshold was applied across all images that matched the staining, yet enabled pixels to be defined as positive/negative in the red (Pcna) channel. The blue (DAPI) channel was used to identify GC nuclei and the proportion of Pcna-positive GCs per follicle was determined. To quantify gH2ax expression in oocytes, the area of the oocyte nucleus was measured from the blue (DAPI) channel and the mean pixel intensity of the corresponding green (gH2ax) channel was recorded. Intensity measurements were taken from the same oocyte cytoplasm and subtracted from the mean nuclear intensity in order to generate a normalised nuclear intensity value for each oocyte. Each protein was analysed in different sections to accommodate the different staining protocols. For all experiments, all follicles were numbered consecutively for analysis to avoid double-counting and all images were independently coded (blinded) to the observer to avoid bias.

2.6. RNA-seq library preparation

Total RNA was isolated from individual cultured ovaries (n) using RNeasy Micro Kits (Qiagen), which included a DNA digestion step. Concentration of each RNA sample (n=6 controls and n=6 exposed to 45 ng/ml nicotine) was assessed using a Qubit Fluorometer and RNA High Sensitivity (HS) Assay Kit (ThermoFisher). RNA-seq libraries were generated using NEBNext Ultra Directional RNA Library Prep Kit with NEBNext Poly(A) mRNA magnetic isolation beads and NEBNext Multiplex Oligos for Illumina according to manufacturer's instructions (New England Biolabs, Herts, UK). Briefly, cDNA was reverse transcribed from >50 ng RNA and whole transcriptome amplification was carried out. Amplified cDNA products were purified using Mag-Bind Total Pure NGS beads (VWR) and quantified using Qubit dsDNA HS assay kit (ThermoFisher). Samples were pooled for 100 bp single end lane sequencing on a P3 NextSeq 2000 sequencer (Illumina).

2.7. RNA-seq analysis

Raw sequencing data were demultiplexed and uploaded to Galaxy (http://usegalaxy.org). Each data file was quality checked using the FastQC protocol and adapter sequences removed using CutAdapt. Trimmed sequences were converted into Sanger reads using FastQ Groomer and aligned to the mouse mm10 genome using the HISAT2 tool. A mean of 86.8 % (control) and 87.4 % (nicotine) reads uniquely mapping and mean of 32936003 (control) and 30320593 (nicotine) reads/sample were generated. RNA quantification was determined with HTSeq Count and RNA read counts were normalised by RNA length (reads per kilobase; RPK) and then by read depth (transcripts per million; TPM). Normalised HTSeq Counts (reads per kilobase per million mapped reads; RPKM) were used to perform differential gene analysis by DESeq2 where values were evident in all samples across one or both groups (Suppl. Table 2). Gene Set Enrichment Analysis (GSEA) was undertaken using the GSEA R Package (Suppl. Table 3). The normalised HTSeq Count data was ranked by fold change and tested using a predefined set of genes (genes sharing the same GO category) to determine if the members of the defined list were scattered throughout the ranked HTSeq Count data or were located primarily at the extremes of this list. An enrichment score was calculated which reflects the extent to which the predefined set of genes was overrepresented at the extremes of the ranked list, the significance of this enrichment score was adjusted to account for multiple testing.

2.8. Statistical analysis

All quantitative data from imaging and qPCR were initially tested for normality using a Kolmogorov-Smirnov test. Imaging outputs were subjected to a Kruskal-Wallis with a Dunn's post-hoc test, and qPCR data were subjected to an ANOVA with a Tukey's post-hoc test. All statistical analyses for imaging and qPCR were carried out using GraphPad Prism (v10). Differences between groups were considered significant if $P<0.05$. For RNA-seq data, differential expression and GSEA were analysed in R as described. Outputs were considered significant where the adjusted p-value (false discovery rate; FDR) <0.05.

3. Results

3.1. Expression of nAChR transcripts in neonatal mouse ovary

Five candidate nAChR genes were analysed in ovaries obtained from PND4, 8 and 16 mice.

Mean levels of the alpha-type receptor transcripts, including *Chrna4, Chrna5* and *Chrna7* were all significantly decreased in PND8 and PND16 ovaries relative to PND4 (Fig. 1**A**). Similarly, for the beta-type receptors, *Chrnb2* was lower in PND16 ovaries and *Chrnb4* was lower in both PND8 and PND16 ovaries relative to PND4 (Fig. 1**B**). Since levels of all nAChR transcripts exhibited a relative decrease in older ovaries, expression of anti-Müllerian hormone (*Amh*) (which is negligible in PFs and highly expressed in early growing follicles (Durlinger et al., 2002)), was also analysed as a sample validation control. The mean level of *Amh* was significantly increased in PND8 and PND16 ovaries relative to PND4 (Fig. 1**B**). The findings that nAChR transcripts are relatively increased in PND4 ovaries densely populated with PFs suggests that nicotine signalling is plausible in these tissues.

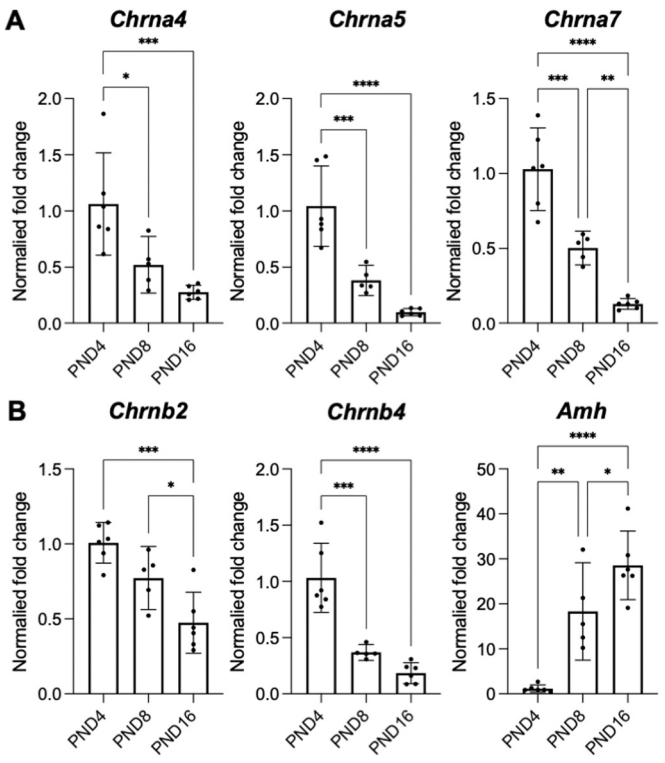

Fig. 1. Relative expression of nAChR transcripts in immature mouse ovaries. RNA was isolated from whole mouse ovaries at PND4, PND8 and PND16 and analysed by qPCR. A) Expression of alpha-type nAChR transcripts – *Chrna4*, *Chrna5*, *Chrna7*. B) Expression of beta-type nAChR transcripts – *Chrnb2*, *Chrnb4* alongside *Amh* as a sample validation control. All data was normalised to the internal reference transcript *Hprt1*. Individual points represent an individual ovary. Bars are means ± 95 %CI. *P<0.05, **P<0.01, ***P<0.001, ****P<0.0001 – Tukey's multiple comparisons test.

3.2. Effect of nicotine and cotinine on morphology of primordial and early growing follicles

Next, neonatal (PND4) mouse ovaries were cultured in a range of concentrations of nicotine or cotinine for 7 days. Localisation of the oocyte-specific protein Ddx4 alongside the granulosa cell-expressed proteins Smad2/3 facilitated identification and staging of follicles for morphometric analysis within a single mid-section from each ovary. Follicles were selected for measurement when a clearly identifiable oocyte nucleus was visible (Fig. 2**A**). A total of 1671 follicles were measured across 27 ovaries for the nicotine experiment and 1189 follicles were measured across 35 ovaries for the cotinine experiment (Suppl. Tables 4–5). Although serial sections were generated, it was not possible to determine absolute number of follicles under each of the treatment conditions due to the variable quality of sections obtained. However, based on the number of eligible follicles sampled from a single mid-section from each ovary, there were no differences between the number or proportion of primordial, transitional or growing follicles between treatment groups for nicotine or cotinine (Fig. 2**B-E**).

Next, the area (μm^2) of all sampled follicles exposed to different concentrations of nicotine was measured. All follicles sampled were manually classified as either primordial (non-growing), transitional, or early growing. When the effect of nicotine was analysed within these follicle stages, the mean overall size of primordial follicles was reduced in ovaries exposed to 15 ng/ml and 45 ng/ml relative to controls ($P<0.001$), but not in the 5 ng/ml group. Likewise, the mean overall size of transitional follicles was reduced in ovaries exposed to 15 ng/ml and 45 ng/ml relative to controls ($P<0.05$), but not in the 5 ng/ml group. Nicotine had no observable effects on the mean size of early growing follicles (Fig. 3**A**).

To determine the cell-specific effects of nicotine in small follicles, individual GC and oocyte compartments were analysed. The mean GC area was reduced in primordial follicles exposed to 15 ng/ml and 45 ng/ml nicotine ($P<0.01$ vs control), but not in the 5 ng/ml group. Likewise, the mean GC area was reduced in transitional follicles exposed to 45 ng/ml nicotine ($P<0.01$ vs control), but not in the 5 ng/ml or 15 ng/ml groups. Nicotine had no observable effects on the mean GC area of early growing follicles (Fig. 3**B**). Similar to GCs, the mean oocyte area was reduced in primordial follicles exposed to 15 ng/ml and 45 ng/ml nicotine ($P<0.01$ vs control), but not in the 5 ng/ml group. Likewise, the mean oocyte area was reduced in transitional follicles exposed to 15 ng/ml and 45 ng/ml nicotine ($P<0.01$ vs control), but not in the 5 ng/ml group. Nicotine had no observable effects on the mean oocyte area of early growing follicles (Fig. 3**C**).

In comparison, when sections were analysed from ovaries exposed to cotinine, none of the concentrations (0–300 ng/ml) caused any observable effect on the overall follicle area, GC area or oocyte area in primordial, transitional and growing follicles (Fig. 4**A-C**). Based on the observable and significant effects of nicotine but not cotinine on small follicle phenotype, subsequent analyses focussed on nicotine alone.

3.3. Effect of nicotine on GC proliferation and apoptosis

Pcna was localised in sections of ovaries exposed to different concentrations of nicotine to determine the effect on GC proliferation (Fig. 5**A**). The proportions of Pcna-positive GCs in primordial, transitional or growing follicles were unaffected by nicotine exposure (Fig. 5**B**).

Sections were also stained for active caspase-3 as a marker of apoptosis. Active caspase-3 was detected in some inter-follicular cells and a small number of granulosa cells. No staining was observed in any primordial follicles. One positive oocyte from a transitional-staged follicle was observed in a control section (0 ng/ml nicotine) and one in a section from the 45 ng/ml nicotine group (Fig. 5**C**). Given the limited number of positively stained cells across all sections, active caspase-3 expression was not quantified between the different nicotine concentration groups. Transcript levels of the pro-apoptosis gene *Bax*, the anti-apoptosis gene *Bcl2* and *Amh* (expressed in GCs of healthy early growing follicles), were all unchanged in ovaries exposed to different concentrations of nicotine (Fig. 5**D**).

3.4. Effect of nicotine on oocyte quality

To determine the effects of nicotine on oocyte quality, gH2AX – an indicator of DNA damage and repair, was localised in sections of cultured ovaries (Fig. 6**A**). Exposure to nicotine caused a significant increase in the intensity of gH2AX in primordial oocytes, at all concentrations (P<0.01 vs control). Nicotine had no effect on gH2AX expression in oocytes of transitional or growing follicles (Fig. 6**B**).

3.5. Effect of nicotine on gene expression in cultured ovaries

Lastly, RNA-seq was used to analyse the transcriptome of ovaries cultured for 7 days in the presence or absence of 45 ng/ml nicotine. This concentration was selected on the basis that it consistently induced a significant reduction in GC and oocyte area in primordial and transitional follicles (Fig. 3). 11,354 unique transcripts were detected in all ovaries of either the control (n=6) or nicotine (n=6) groups. From this sub-set, 68 transcripts were differentially expressed between the two groups, of which 6 were significantly decreased and 62 were increased in the nicotine samples relative to the controls (FDR<0.05; Fig. 7**A-B**). Differentially expressed (DE) transcripts were manually curated on the basis of gene ontology biological process (GO BP) and classified accordingly. Notably, a number of DE transcripts were associated with DNA damage response, mitosis, differentiation and morphogenesis,

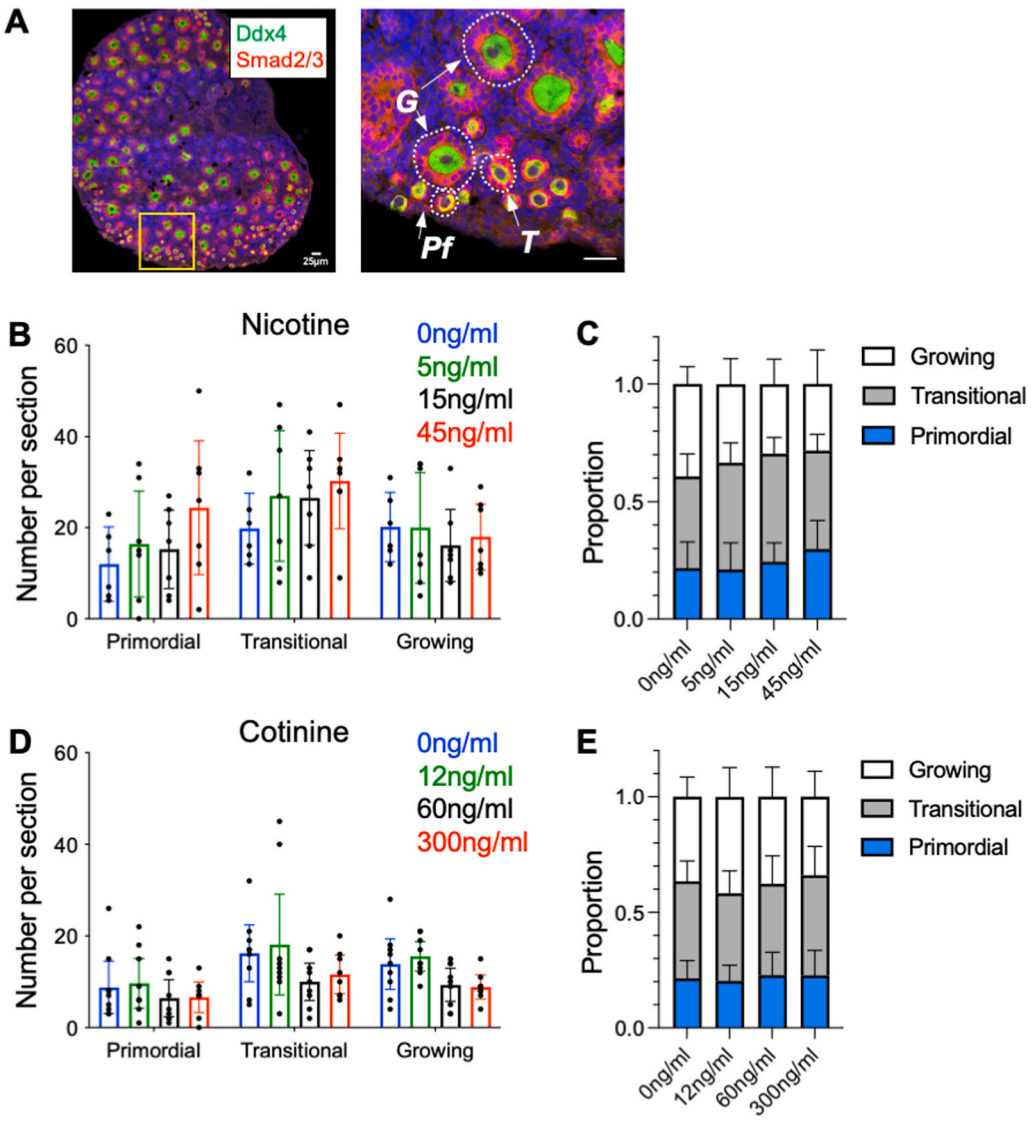

Fig. 2. Effect of nicotine and cotinine on number and proportion of small follicles from cultured neonatal mouse ovaries. A) Mid-sections of ovaries were labelled using antibodies against Ddx4 (green) and Smad2/3 (red) to facilitate identification of oocytes and GCs, respectively. Cell nuclei were counterstained with DAPI (blue). The panel on the right is a magnified image of the yellow inset. Examples of follicles classified as primordial (*Pf*), transitional (*T*) and growing (G) as defined in the methods. B) Number of follicles at each classified stage that met sampling criteria (see methods) from ovaries cultured in different concentrations of nicotine. C) Proportion of follicles sampled at each stage within each nicotine group. D) Number of follicles at each classified stage that met sampling criteria from ovaries cultured in different concentrations of cotinine. E) Proportion of follicles sampled at each stage within each cotinine group. Individual points represent an individual section from a single ovary. All bars are means ± 95 %CI.

neuronal activity, RNA processing and transcription, protein binding and transport, ion homeostasis and transport, immune function and carbohydrate metabolism among others (Fig. 7**C**). GSEA, which considers all 11,354 transcripts and assigns a weighting based on fold change, identified 446 activated and 105 suppressed GO BPs in the nicotine treated ovaries relative to the controls (Suppl. Table 4). All 551 of these were manually assigned into 24 key themes, with the frequency of GO BPs within each category listed. Several consistent themes were identified between the GSEA and DE analysis – additionally revealing that neuron function and synapse activity, cell morphogenesis and differentiation, were suppressed by nicotine exposure. Conversely, biological processes related to cell stress, RNA processing, lipid metabolism, immune response and other cell responses were activated. GSEA additionally identified meiosis, cell adhesion and ECM as being suppressed, and apoptosis, autophagy, respiration and mitochondrial activity as activated in nicotine treated ovaries (Fig. 7**D**). A representative GO BP from each of these themes was plotted to indicate the relative gene ratios (Fig. 7**E**).

4. Discussion

The overall aim of this study was to investigate the effects of nicotine and cotinine on the ovarian reserve in mice. Transcripts for a range of nAChRs were expressed in PND4 mouse ovaries densely populated with primordial follicles, suggesting a mechanism whereby nicotine and/or cotinine can signal. To study this further, PND4 ovaries were cultured with either nicotine or cotinine, at a range of concentrations consistent with published plasma levels of e-cigarette users. Neither nicotine nor cotinine caused any observable differences in the total number of primordial, transitional or early growing follicles. Cotinine had no further observable effects on morphological features of small follicles; however, with nicotine, a small reduction in GC and oocyte size was observed in primordial and transitional staged follicles at both 15 ng/ml and 45 ng/ml. Although this finding was not associated with changes in GC

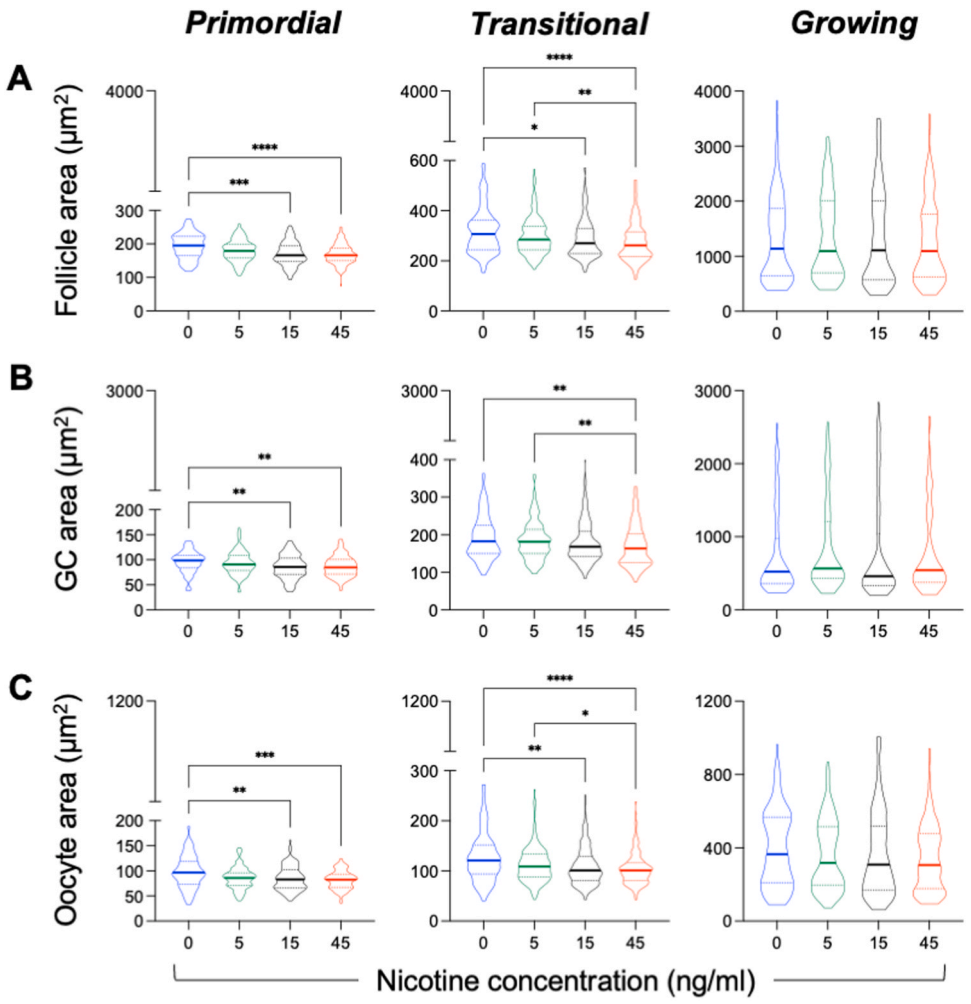

Fig. 3. Stage-specific effect of nicotine on size parameters of small follicles from cultured neonatal mouse ovaries. Follicles were classified as primordial, transitional or growing based on morphological phenotype as described in the methods. A) Effect of nicotine concentration on follicle area. B) Effect of nicotine concentration on GC area. C) Effect of nicotine concentration on oocyte area. Solid and dashed lines within violin plots indicate medians and interquartile ranges, respectively. *P<0.05, **P<0.01, ***P<0.001, ****P<0.0001 – Dunn's multiple comparisons test.

proliferation or apoptosis, we found nicotine exposure was associated with elevated gH2AX expression in oocytes of primordial follicles – suggesting an effect on DNA damage and repair. Using RNA-seq, we identified 68 transcripts that were differentially regulated in ovaries exposed to nicotine. GSEA as well as ontological analyses of differentially expressed genes revealed significant associations with biological processes including elevated DNA damage, respiration and immune function, alongside suppression of meiosis, cell adhesion, differentiation and morphogenesis. These processes are likely to impinge on the overall quality of the ovarian reserve.

Nicotine signals through nAChRs, which are typically expressed in the central and peripheral nervous system, although their localisation and activity in other non-neuronal cell types is now more evident (Albuquerque et al., 2009, Urra et al., 2016). We initially analysed the expression of common nAChR sub-type transcripts in pre-pubertal mouse ovaries and found that *Chrna4*, *Chrna5*, *Chrna7*, *Chrnb2* and *Chrnb4* were all relatively higher in PND4 ovaries compared with older ovaries. At PND4, mouse ovaries are densely populated with primordial follicles, while at PND8 and PND16, successive stages of early growing follicles predominate, and the proportion of primordial follicles declines (Fenwick et al., 2011, Granados-Aparici et al., 2019). The relative decrease of all five nAchR transcripts through these early age groups, suggests a strong association with primordial follicles. Other recent studies have also reported expression of these transcripts in fetal and neonatal mouse ovaries (Liu et al., 2020, Mourikes et al., 2024, Wang et al., 2018), with further localisation of Chrna4 and Chrna7 transcripts and proteins to granulosa cells and oocytes of primordial follicles (Mourikes et al., 2024). Thus, it is plausible that nicotine can exert direct effects on primordial follicles through these receptors.

Nicotine is the main ingestible component of e-cigarettes and is detectable at a range of plasma concentrations in users between 1 and 50 ng/ml (Dawkins and Corcoran, 2014, Farsalinos et al., 2015, Vansickel and Eissenberg, 2013). In our study we exposed ovaries *in vitro* to a range of concentrations of nicotine considered to be reflective of low (5 ng/m), medium (15 ng/ml) and high (45 ng/ml) plasma levels. Following histological evaluation, we did not observe any differences in the absolute number or proportion of follicles. Previous studies investigating the effects of nicotine in neonatal or adult rodents by direct i.p. administration have observed a slight, but significant reduction in primordial follicles – although the concentrations used were much higher (1–5 mg/kg) (Sezer et al., 2020, Wang et al., 2018). By comparison, Faghani et al. (2022), administered 0.6 mg/kg to adult mice and although this concentration was still higher than the doses we have used, there was no observable effects of nicotine on primordial follicle number in their study. Therefore, it is likely that concentrations of nicotine used and the time of exposure (7 days) in our study were not sufficient to induce PF loss.

The lack of any effect of nicotine on PF number is also consistent with

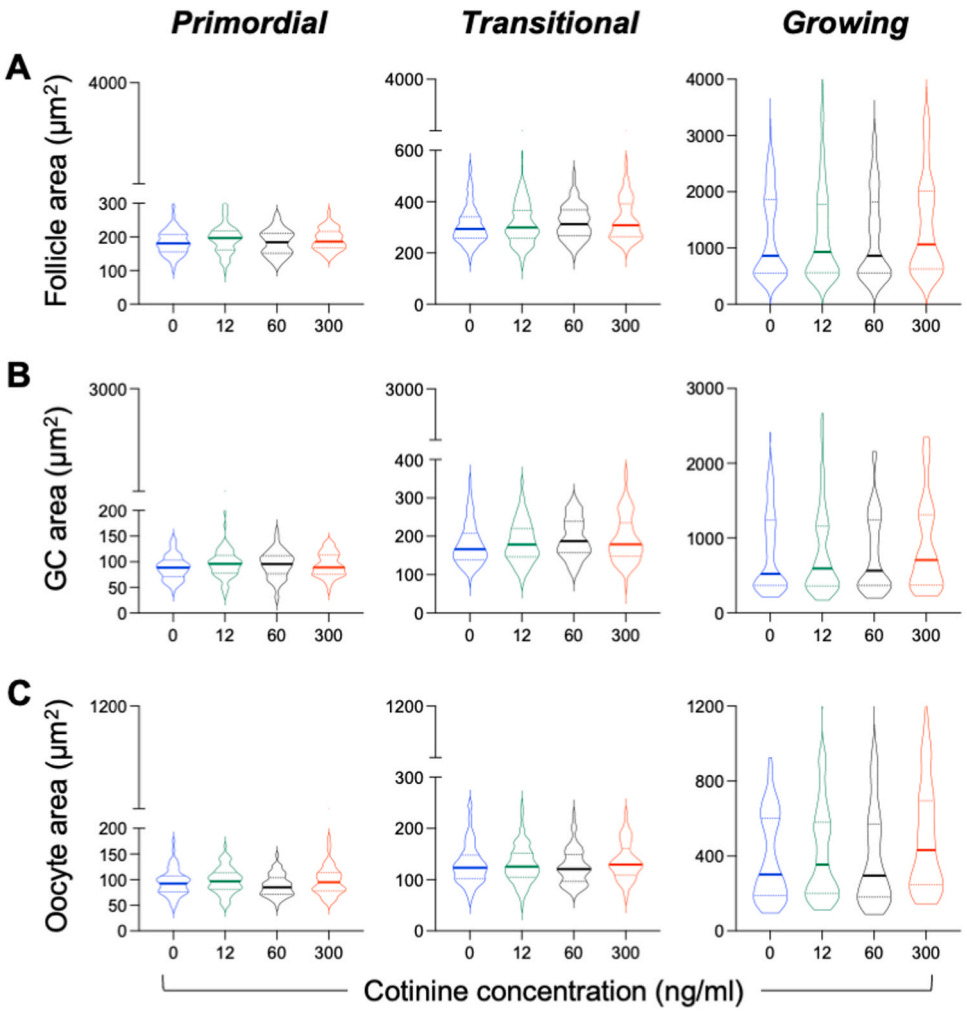

Fig. 4. Stage-specific effect of cotinine on size parameters of small follicles from cultured neonatal mouse ovaries. Follicles were classified as primordial, transitional or growing based on morphological phenotype as described in the methods. A) Effect of cotinine concentration on follicle area. B) Effect of cotinine concentration on GC area. C) Effect of cotinine concentration on oocyte area. Solid and dashed lines within violin plots indicate medians and interquartile ranges, respectively. No differences were observed between treatment groups for any of the parameters displayed ($P>0.05$; Kruskal-Wallis).

the limited evidence for apoptosis in cultured ovaries. Active caspase-3, which is expressed in atretic follicles (Fenwick and Hurst, 2002), was detectable in a few GCs and a single oocyte and expression of *Bcl2/Bax* was unchanged in the nicotine treated groups when compared to controls. In one study, intraperitoneal injection of nicotine in adult rats caused apoptosis of GCs of growing follicles, but apoptosis was undetectable in PFs (Sezer et al., 2020). In our sequencing analysis, nicotine caused an increase in *Snai2* and *Nudt2*, genes involved in epithelial – mesenchymal transition (Casas et al., 2011, Hidmi et al., 2023) along with *Nme3,* which has a role in DNA damage and repair (Tsao et al., 2016). All three genes are also associated with apoptosis regulation (Bailey et al., 2002, Wu et al., 2005) and GSEA analysis identified 20 significantly activated GO BPs that were attributed to apoptosis and cell death; however, some of these associations were specifically related to neurons (Suppl. Table 4). Nicotine has also been shown to promote autophagy during the period of follicle formation and in somatic cells of growing follicles (Liu et al., 2020, Liu et al., 2021, Sezer et al., 2020, Wang et al., 2018, Zhou et al., 2024). Although we did not detect any DE transcripts associated with autophagy, GSEA identified 5 activated GO BPs, suggesting autophagy is also evident in our model. Data from the RNA-seq therefore indicates that cells within the ovaries exposed to nicotine are poised to execute apoptosis or autophagy; however, given the lack of evidence for follicle loss, it is also possible that this finding relates to non-follicular cells.

Interestingly, the medium and high concentrations of nicotine caused small, but significant reductions in PF and transitional follicle size. Further analysis revealed that this was due to a reduction in oocyte size with both concentrations, and additionally a reduction in GC size in the high concentration group. As GC size was determined from measurements of area, we therefore considered whether there was a change in GC proliferation. The proportion of Pcna-positive GCs per follicle, as well as the mean number of GCs per follicle (**Suppl.** Fig. 1) did not vary between groups exposed to different concentrations of nicotine within primordial, transitional and growing follicles. Moreover, levels of *Amh*, a proxy indicator of GC number in growing follicles, was also unchanged. Faghani et al., (2022), similarly did not detect any effect of nicotine on the proliferative index (measured by Ki67 staining) of GCs in PFs in adult mice. With the sequencing data, *Kif2b*, a gene involved in chromosome segregation in mitotic cells (Shrestha and Draviam, 2013), was reduced in nicotine treated ovaries and *Rprm*, known to have a role in G2 arrest (Ohki et al., 2000) was increased. Aside from this, there was no indication from the GSEA analysis that cell division or proliferation was affected by nicotine. It is therefore likely that the observed change in GC area was due to a reduction in GC compartment size rather than GC number. It is unclear how this altered phenotype relates to follicle development, although it is noteworthy that several genes involved in differentiation and morphogenesis processes were differentially regulated in response to nicotine. For example, *Krt80*, *Setd2* and *Speg*, which

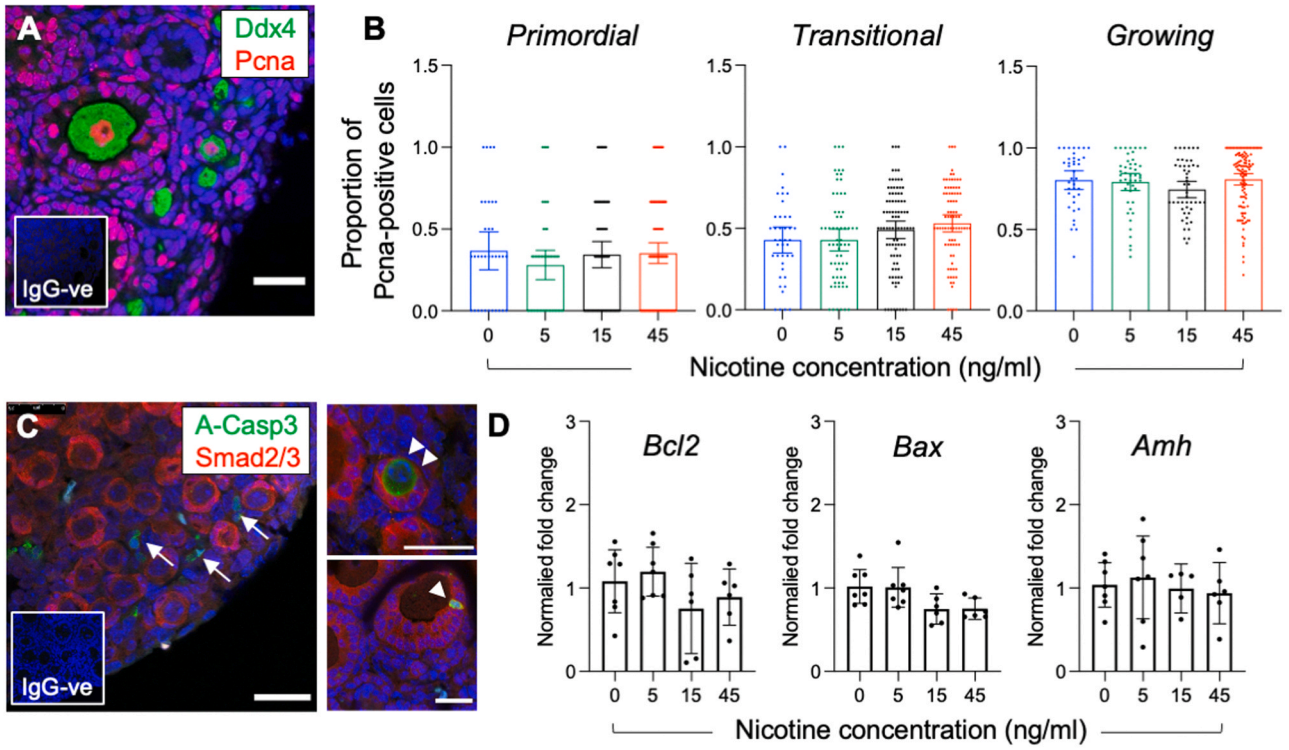

Fig. 5. Stage-specific effect of nicotine on cell proliferation and apoptosis in small follicles from cultured neonatal mouse ovaries. A) Sections of ovaries labelled using antibodies against Ddx4 (green) and Pcna (red) to facilitate identification of oocytes and proliferative GCs, respectively. Cell nuclei are counterstained with DAPI (blue). B) Effect of nicotine concentration on Pcna expression in primordial, transitional and early growing follicles. Bars indicate mean proportion of Pcna-positive GCs per follicle (±95 % CI). C) Sections of ovaries labelled using antibodies against Smad2/3 (red) and Active caspas-3 (green) to facilitate identification of GCs and apoptotic cells, respectively. Cell nuclei are counterstained with DAPI (blue). Examples of active caspase-3 positive inter-follicular cells (arrows), an oocyte (double arrowhead) and a GC (single arrowhead) are indicated. Scale bars = 25 μm. D) Relative expression of *Bax*, *Bcl2* and *Amh* transcripts in ovaries exposed to different concentrations of nicotine by qPCR. Data was normalised to the internal reference transcript *Atp5b*. Individual points represent an individual ovary. Bars are means ± 95 %CI.

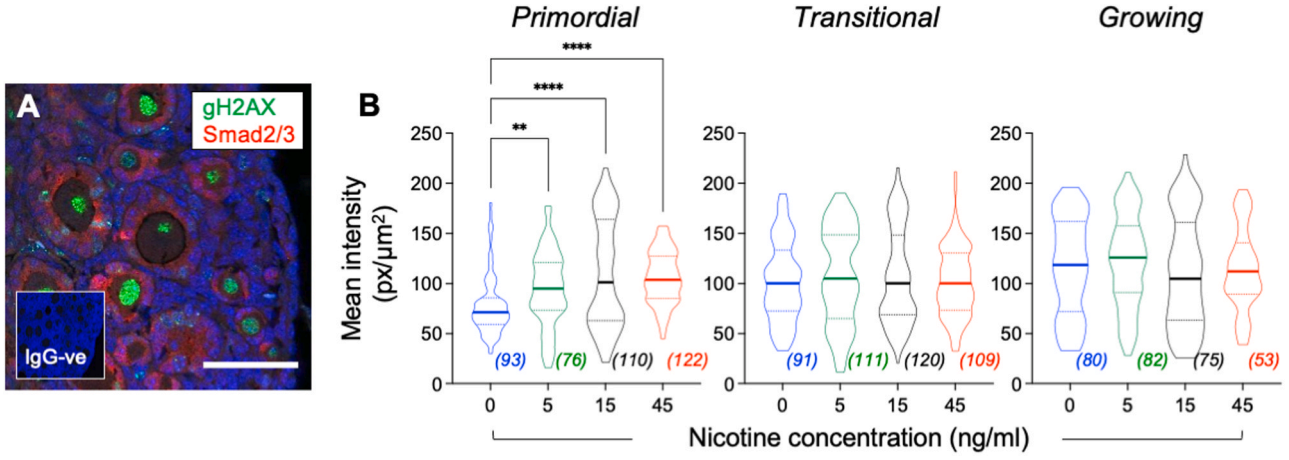

Fig. 6. Stage-specific effect of nicotine on oocyte DNA quality in small follicles from cultured neonatal mouse ovaries. A) Sections of ovaries were labelled using antibodies against gH2AX (green) and Smad2/3 (red; to highlight GCs). Cell nuclei are counterstained with DAPI (blue). B) Effect of nicotine concentration on gH2AX expression in oocyte nuclei of primordial, transitional and early growing follicles. Solid and dashed lines indicate medians and interquartile ranges, respectively. The number of follicles sampled for each group are indicated in parentheses. **P<0.01, ****P<0.0001 – Dunn's multiple comparisons test.

have roles in cytoskeletal organisation and *Snai2* and *Tmem198*, which are both involved in Wnt-regulated cell development were increased relative to the control group (Casas et al., 2011, Liang et al., 2011). Manual curation from the GSEA identified numerous GO BPs relating to cell adhesion and ECM, as well as cell morphogenesis, differentiation and development (e.g. actin cytoskeleton organisation) that were all suppressed by nicotine. Thus, nicotine impacts cell development in these ovaries, although further investigations would be needed to reveal the follicle-specific targets.

The observed reduction in oocyte size also indicates these cells are sensitive to nicotine exposure. Interestingly, the increase in gH2AX staining intensity in oocyte nuclei of PFs provides further evidence of this. Gamma H2AX is a phosphorylated histone protein that often forms when double strand breaks appear (Mah et al., 2010). Recent studies

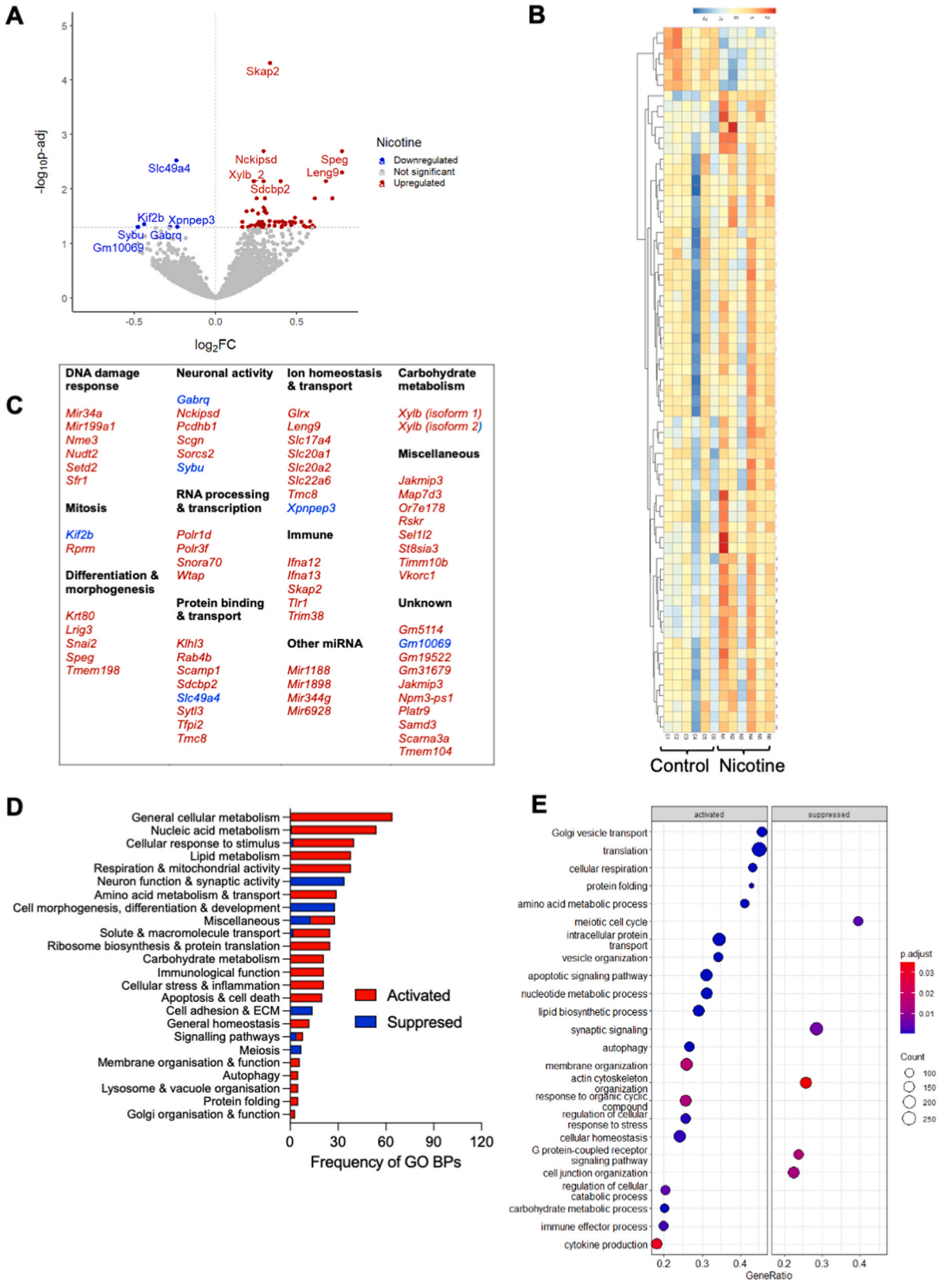

Fig. 7. Differential expression analysis of the transcriptome of cultured neonatal mouse ovaries exposed to nicotine. Individual ovaries were maintained in normal culture media either in the absence (control; n=6) or presence of 45 ng/ml nicotine (n=6) for seven days. Samples were processed and analysed by RNA-seq. A) Volcano plot showing up- and down-regulated transcripts (top 6 in each labelled) in nicotine treated ovaries relative to control. B) Heatmap showing clustering of 68 differentially expressed transcripts between individual control and nicotine treated ovaries (FDR<0.05). C) List of differentially expressed transcripts (gene symbols) manually classified by GO biological process. Transcripts listed in red were significantly increased and those in blue were decreased in the nicotine treated ovaries relative to controls. D) Manual curation of GSEA analysis summarising 551 significant associations with GO BPs. E) Scatterplot from GSEA output indicating selected GO BPs relating to the manual curation analysis.

have found gH2AX is elevated following nicotine exposure in mouse and human oocytes undergoing meiotic arrest during follicle formation (Cheng et al., 2018, Liu et al., 2020). In line with this, we identified several nicotine-induced transcripts that have roles in DNA damage and double strand break repair, including the aforementioned *Nme3* and *Nudt2*, along with *Mir34a, Setd2* and *Sfr1* (Bailey et al., 2002, Carvalho et al., 2014, Cerna et al., 2019, Yuan and Chen, 2011). These findings indicate that exposure to nicotine can impact the integrity of oocyte DNA and although other ovarian cells may be impacted, it was interesting to note that a significant association relating to suppression of meiosis was identified by GSEA.

The relative reduction in oocyte and GC size in PFs and transitional follicles exposed to nicotine could also be related to metabolic and stress-induced alterations in homeostasis. In particular, the majority of significant GO BPs from the GSEA related to themes including general cellular metabolism, stress and inflammation, respiration and mitochondrial activity and lipid metabolism, among others. Elevated lipid peroxidation and altered mitochondrial function has been observed in rodent GCs exposed to nicotine (Liu et al., 2020, Sezer et al., 2020). The many GO BPs attributed to cellular respiration and mitochondrial function in our study indicates that nicotine causes a change in energy metabolism within the PND4 ovary.

In addition to oocytes and GCs, there are numerous other cell types in the ovary that may be susceptible to nicotine. The ovary is replete with nerves that are known to regulate follicle development and steroidogenesis (Cuevas et al., 2022). The differentially expressed genes associated with neuronal activity (*Gabrq, Nckipsd, Pcdhb1, Scgn, Sorcs2, Sybu*) as well as the many GO BPs associated with synaptic activity are unsurprising given the well-established effects of nicotine on neuronal function (Albuquerque et al., 2009). Likewise, several genes with a role in immune function were increased in response to nicotine. Although some of these may be expressed in GCs (e.g. Tlr1; (Xie et al., 2020)), others, such as *Ifna*, *Skap2* and *Trim38* are typically expressed in macrophages and lymphocytes (Hu and Shu, 2017, Swiecki et al., 2011, Wilmink and Spalinger, 2023); therefore, the effect of nicotine on other cells that have key roles regulating ovarian function are yet to be investigated.

As well as nicotine, we also analysed the effect of cotinine on the ovarian reserve. Cotinine is a product of nicotine metabolism and is detectable in plasma of e-cigarette users at approximately 1–300 ng/ml with a half-life of 19–24 h (Benowitz et al., 1983, Flouris et al., 2013). In humans, cotinine is readily detectable in follicular fluid, indicating this metabolite can accumulate in the ovary and therefore potentially exert an influence on surrounding cells (Zenzes et al., 1997, Zenzes and Reed, 1998). In our study we exposed ovaries *in vitro* to a range of concentrations of cotinine considered to be reflective of low (12 ng/m), medium (60 ng/ml) and high (300 ng/ml) plasma levels. Compared with nicotine, cotinine had no effect on any morphological measures of small follicles, including oocyte and GC size, and therefore further analyses were not carried out. Other studies have reported that cotinine has no effect on steroidogenesis in cultured GCs and theca from a range of species (Blackburn et al., 1994, Sanders et al., 2002). Cotinine acts as a weak agonist reported to be 100x less potent than nicotine and exhibits limited toxicity in a range of cell models (Moran, 2012). Therefore, it is unlikely that cotinine has a major impact on the ovarian reserve.

In summary, we have used a PND4 mouse ovary as a model to investigate the effects of nicotine on the ovarian reserve. Although it is recognised that mouse tissues may respond differently to human, the key message from this study is that exposure of ovaries over a 7-day period to nicotine across a range of concentrations consistent with plasma levels in e-cigarette users leads to subtle, but measurable effects on the ovarian reserve. In particular, the smallest primordial and transitional stage follicles are susceptible to nicotine in a way that promotes intrinsic molecular events that reflect an impact on oocyte quality. Given that these follicles must remain viable throughout the reproductive lifetime means that the true impact of nicotine and e-cigarette usage may not be realised until these follicles are required to develop and produce steroid hormones and ultimately yield a high-quality oocyte for ovulation and fertilisation.

CRediT authorship contribution statement

Sara M. Idrees: Writing – review & editing, Visualization, Validation, Methodology, Investigation, Funding acquisition, Formal analysis, Data curation, Conceptualization. **Sarah L. Waite:** Writing – review & editing, Visualization, Validation, Supervision, Software, Methodology, Investigation, Formal analysis, Data curation. **Sofia Granados Aparici:** Writing – review & editing, Supervision, Resources, Project administration, Methodology, Investigation. **Mark A. Fenwick:** Writing – review & editing, Writing – original draft, Visualization, Validation, Supervision, Resources, Project administration, Methodology, Investigation, Formal analysis, Data curation, Conceptualization.

Declaration of Competing Interest

The authors declare the following financial interests/personal relationships which may be considered as potential competing interests: Sara Idrees reports financial support was provided by Royal Embassy of Saudi Arabia Cultural Bureau in London. If there are other authors, they declare that they have no known competing financial interests or personal relationships that could have appeared to influence the work reported in this paper.

Acknowledgements

The authors would like to thank Ms Orla Gallagher from the skelet. AL laboratory (Mellanby Centre for Bone Research, University of Sheffield) for technical support with histology. This work was supported by funds received from the Royal Embassy of Saudi Arabia Cultural Bureau (SACB) awarded to S.M.I. and the University of Sheffield Institutional Open Access fund.

Appendix A. Supporting information

Supplementary data associated with this article can be found in the online version at doi:10.1016/j.ecoenv.2024.117302.

Data Availability

Data will be made available on request.

References

Albuquerque, E.X., Pereira, E.F., Alkondon, M., Rogers, S.W., 2009. Mammalian nicotinic acetylcholine receptors: from structure to function. Physiol. Rev. 89, 73–120.
Bailey, S., Sedelnikova, S.E., Blackburn, G.M., Abdelghany, H.M., Baker, P.J., Mclennan, A.G., Rafferty, J.B., 2002. The crystal structure of diadenosine tetraphosphate hydrolase from Caenorhabditis elegans in free and binary complex forms. Structure 10, 589–600.
Blackburn, C.W., Peterson, C.A., Hales, H.A., Carrell, D.T., Jones, K.P., Urry, R.L., Peterson, C.M., 1994. Nicotine, but not cotinine, has a direct toxic effect on ovarian function in the immature gonadotropin-stimulated rat. Reprod. Toxicol. 8, 325–331.
Carvalho, S., Vitor, A.C., Sridhara, S.C., Martins, F.B., Raposo, A.C., Desterro, J.M., Ferreira, J., Almeida, S. F, D.E., 2014. SETD2 is required for DNA double-strand break repair and activation of the p53-mediated checkpoint. Elife 3, e02482.
Casas, E., Kim, J., Bendesky, A., Ohno-Machado, L., Wolfe, C.J., Yang, J., 2011. Snail2 is an essential mediator of Twist1-induced epithelial mesenchymal transition and metastasis. Cancer Res 71, 245–254.
Cerna, K., Oppelt, J., Chochola, V., Musilova, K., Seda, V., Pavlasova, G., Radova, L., Arigoni, M., Calogero, R.A., Benes, V., Trbusek, M., Brychtova, Y., Doubek, M., Mayer, J., Pospisilova, S., Mraz, M., 2019. MicroRNA miR-34a downregulates FOXP1 during DNA damage response to limit BCR signalling in chronic lymphocytic leukaemia B cells. Leukemia 33, 403–414.
Cheng, S.F., Qin, X.S., Han, Z.L., Sun, X.F., Feng, Y.N., Yang, F., Ge, W., Li, L., Zhao, Y., De Felici, M., Zou, S.H., Zhou, Y., Shen, W., 2018. Nicotine exposure impairs germ cell development in human fetal ovaries cultured in vitro. Aging 10, 1556–1574.
Cuevas, F.C., Bastias, D., Alanis, C., Benitez, A., Squicciarini, V., Riquelme, R., Sessenhausen, P., Mayerhofer, A., Lara, H.E., 2022. Muscarinic receptors in the rat

ovary are involved in follicular development but not in steroid secretion. Physiol. Rep. 10, e15474.
Dawkins, L., Corcoran, O., 2014. Acute electronic cigarette use: nicotine delivery and subjective effects in regular users. Psychopharmacology 231, 401–407.
Dempsey, D., Jacob, P., 3rd, Benowitz, N.L., 2002. Accelerated metabolism of nicotine and cotinine in pregnant smokers. J. Pharm. Exp. Ther. 301, 594–598.
Di Prospero, F., Luzi, S., Iacopini, Z., 2004. Cigarette smoking damages women's reproductive life. Reprod. Biomed. Online 8, 246–247.
Durlinger, A.L., Visser, J.A., Themmen, A.P., 2002. Regulation of ovarian function: the role of anti-Mullerian hormone. Reproduction 124, 601–609.
Dwoskin, L.P., Teng, L., Buxton, S.T., Crooks, P.A., 1999. (S)-(-)-Cotinine, the major brain metabolite of nicotine, stimulates nicotinic receptors to evoke [3H]dopamine release from rat striatal slices in a calcium-dependent manner. J. Pharm. Exp. Ther. 288, 905–911.
Eppig, J.J., O'brien, M.J., 1996. Development in vitro of mouse oocytes from primordial follicles. Biol. Reprod. 54, 197–207.
Faghani, M., Saedi, S., Khanaki, K., Mohammadghasemi, F., 2022. Ginseng alleviates folliculogenesis disorders via induction of cell proliferation and downregulation of apoptotic markers in nicotine-treated mice. J. Ovarian Res. 15, 14.
Farsalinos, K.E., Spyrou, A., Stefopoulos, C., Tsimopoulou, K., Kourkoveli, P., Tsiapras, D., Kyrzopoulos, S., Poulas, K., Voudris, V., 2015. Nicotine absorption from electronic cigarette use: comparison between experienced consumers (vapers) and naive users (smokers). Sci. Rep. 5, 11269.
Fenwick, M.A., Hurst, P.R., 2002. Immunohistochemical localization of active caspase-3 in the mouse ovary: growth and atresia of small follicles. Reproduction 124, 659–665.
Fenwick, M.A., Mansour, Y.T., Franks, S., Hardy, K., 2011. Identification and regulation of bone morphogenetic protein antagonists associated with preantral follicle development in the ovary. Endocrinology 152, 3515–3526.
Findlay, J.K., Hutt, K.J., Hickey, M., Anderson, R.A., 2015. What is the "ovarian reserve"? Fertil. Steril. 103, 628–630.
Flouris, A.D., Chorti, M.S., Poulianiti, K.P., Jamurtas, A.Z., Kostikas, K., Tzatzarakis, M. N., Wallace Hayes, A., Tsatsakis, A.M., Koutedakis, Y., 2013. Acute impact of active and passive electronic cigarette smoking on serum cotinine and lung function. Inhal. Toxicol. 25, 91–101.
Furlong, H.C., Stampfli, M.R., Gannon, A.M., Foster, W.G., 2015. Cigarette smoke exposure triggers the autophagic cascade via activation of the AMPK pathway in mice. Biol. Reprod. 93, 93.
Gannon, A.M., Stampfli, M.R., Foster, W.G., 2012. Cigarette smoke exposure leads to follicle loss via an alternative ovarian cell death pathway in a mouse model. Toxicol. Sci. 125, 274–284.
Granados-Aparici, S., Hardy, K., Franks, S., Sharum, I.B., Waite, S.L., Fenwick, M.A., 2019. SMAD3 directly regulates cell cycle genes to maintain arrest in granulosa cells of mouse primordial follicles. Sci. Rep. 9, 6513.
Hammond, D., Rynard, V.L., Reid, J.L., 2020. Changes in Prevalence of Vaping Among Youths in the United States, Canada, and England from 2017 to 2019. JAMA Pedia 174, 797–800.
Hardy, K., Mora, J.M., Dunlop, C., Carzaniga, R., Franks, S., Fenwick, M.A., 2018. Nuclear exclusion of SMAD2/3 in granulosa cells is associated with primordial follicle activation in the mouse ovary. J. Cell Sci. 131.
Harlow, B.L., Signorello, L.B., 2000. Factors associated with early menopause. Maturitas 35, 3–9.
Hidmi, S., Nechushtan, H., Razin, E., Tshori, S., 2023. Role of Nudt2 in anchorage-independent growth and cell migration of human melanoma. Int J. Mol. Sci. 24.
Hu, M.M., Shu, H.B., 2017. Multifaceted roles of TRIM38 in innate immune and inflammatory responses. Cell Mol. Immunol. 14, 331–338.
Jurisicova, A., Taniuchi, A., Li, H., Shang, Y., Antenos, M., Detmar, J., Xu, J., Matikainen, T., Benito Hernandez, A., Nunez, G., Casper, R.F., 2007. Maternal exposure to polycyclic aromatic hydrocarbons diminishes murine ovarian reserve via induction of Harakiri. J. Clin. Invest 117, 3971–3978.
Li, F., Ding, J., Cong, Y., Liu, B., Miao, J., Wu, D., Wang, L., 2020. Trichostatin A alleviated ovarian tissue damage caused by cigarette smoke exposure. Reprod. Toxicol. 93, 89–98.
Li, F., Wang, Y., Xu, M., Hu, N., Miao, J., Zhao, Y., Wang, L., 2022. Single-nucleus RNA Sequencing reveals the mechanism of cigarette smoke exposure on diminished ovarian reserve in mice. Ecotoxicol. Environ. Saf. 245, 114093.
Liang, J., Fu, Y., Cruciat, C.M., Jia, S., Wang, Y., Tong, Z., Tao, Q., Ingelfinger, D., Boutros, M., Meng, A., Niehrs, C., Wu, W., 2011. Transmembrane protein 198 promotes LRP6 phosphorylation and Wnt signaling activation. Mol. Cell Biol. 31, 2577–2590.
Lindson, N., Butler, A.R., Mcrobbie, H., Bullen, C., Hajek, P., Begh, R., Theodoulou, A., Notley, C., Rigotti, N.A., Turner, T., Livingstone-Banks, J., Morris, T., Hartmann-Boyce, J., 2024. Electronic cigarettes for smoking cessation. Cochrane Database Syst. Rev. 1, CD010216.
Liu, W.X., Tan, S.J., Wang, Y.F., Li, L., Sun, X.F., Liu, J., Klinger, F.G., De Felici, M., Shen, W., Cheng, S.F., 2020. Melatonin ameliorates murine fetal oocyte meiotic dysfunction in F1 and F2 offspring caused by nicotine exposure during pregnancy. Environ. Pollut. 263, 114519.
Liu, W.X., Zhang, Y.J., Wang, Y.F., Klinger, F.G., Tan, S.J., Farini, D., De Felici, M., Shen, W., Cheng, S.F., 2021. Protective mechanism of luteinizing hormone and follicle-stimulating hormone against nicotine-induced damage of mouse early folliculogenesis. Front Cell Dev. Biol. 9, 723388.
Livak, K.J., Schmittgen, T.D., 2001. Analysis of relative gene expression data using real-time quantitative PCR and the 2(-Delta Delta C(T)) Method. Methods 25, 402–408.
Mah, L.J., El-Osta, A., Karagiannis, T.C., 2010. gammaH2AX: a sensitive molecular marker of DNA damage and repair. Leukemia 24, 679–686.
Moran, V.E., 2012. Cotinine: beyond that expected, more than a biomarker of tobacco consumption. Front Pharm. 3, 173.
Mourikes, V.E., Santacruz-Marquez, R., Deviney, A., Neff, A., Laws, M.J., Flaws, J.A., 2024. Neonicotinoids differentially modulate nicotinic acetylcholine receptors in immature and antral follicles in the mouse ovary1. Biol. Reprod.
Oboni, J.B., Marques-Vidal, P., Bastardot, F., Vollenweider, P., Waeber, G., 2016. Impact of smoking on fertility and age of menopause: a population-based assessment. BMJ Open 6, e012015.
Ohki, R., Nemoto, J., Murasawa, H., Oda, E., Inazawa, J., Tanaka, N., Taniguchi, T., 2000. Reprimo, a new candidate mediator of the p53-mediated cell cycle arrest at the G2 phase. J. Biol. Chem. 275, 22627-30.
Sanders, S.R., Cuneo, S.P., Turzillo, A.M., 2002. Effects of nicotine and cotinine on bovine theca interna and granulosa cells. Reprod. Toxicol. 16, 795–800.
Sezer, Z., Ekiz Yilmaz, T., Gungor, Z.B., Kalay, F., Guzel, E., 2020. Effects of vitamin E on nicotine-induced lipid peroxidation in rat granulosa cells: Folliculogenesis. Reprod. Biol. 20, 63–74.
Shrestha, R.L., Draviam, V.M., 2013. Lateral to end-on conversion of chromosome-microtubule attachment requires kinesins CENP-E and MCAK. Curr. Biol. 23, 1514–1526.
Sobinoff, A.P., Beckett, E.L., Jarnicki, A.G., Sutherland, J.M., Mccluskey, A., Hansbro, P. M., Mclaughlin, E.A., 2013. Scrambled and fried: cigarette smoke exposure causes antral follicle destruction and oocyte dysfunction through oxidative stress. Toxicol. Appl. Pharm. 271, 156–167.
Swiecki, M., Wang, Y., Vermi, W., Gilfillan, S., Schreiber, R.D., Colonna, M., 2011. Type I interferon negatively controls plasmacytoid dendritic cell numbers in vivo. J. Exp. Med 208, 2367–2374.
Tehrani, H., Rajabi, A., Ghelichi-Ghojogh, M., Nejatian, M., Jafari, A., 2022. The prevalence of electronic cigarettes vaping globally: a systematic review and meta-analysis. Arch. Public Health 80, 240.
Tingen, C., Kim, A., Woodruff, T.K., 2009. The primordial pool of follicles and nest breakdown in mammalian ovaries. Mol. Hum. Reprod. 15, 795–803.
Tsao, N., Yang, Y.C., Deng, Y.J., Chang, Z.F., 2016. The direct interaction of NME3 with Tip60 in DNA repair. Biochem J. 473, 1237–1245.
Tuttle, A.M., Stampfli, M., Foster, W.G., 2009. Cigarette smoke causes follicle loss in mice ovaries at concentrations representative of human exposure. Hum. Reprod. 24, 1452–1459.
Urra, J., Blohberger, J., Tiszavari, M., Mayerhofer, A., Lara, H.E., 2016. In vivo blockade of acetylcholinesterase increases intraovarian acetylcholine and enhances follicular development and fertility in the rat. Sci. Rep. 6, 30129.
Vansickel, A.R., Eissenberg, T., 2013. Electronic cigarettes: effective nicotine delivery after acute administration. Nicotine Tob. Res 15, 267–270.
Wang, Y.F., Sun, X.F., Han, Z.L., Li, L., Ge, W., Zhao, Y., De Felici, M., Shen, W., Cheng, S. F., 2018. Protective effects of melatonin against nicotine-induced disorder of mouse early folliculogenesis. Aging (Albany NY) 10, 463–480.
Weinberg, C.R., Wilcox, A.J., Baird, D.D., 1989. Reduced fecundability in women with prenatal exposure to cigarette smoking. Am. J. Epidemiol. 129, 1072–1078.
Wilmink, M., Spalinger, M.R., 2023. SKAP2-A Molecule at the Crossroads for Integrin Signalling and Immune Cell Migration and Function. Biomedicines 11.
Wu, W.S., Heinrichs, S., Xu, D., Garrison, S.P., Zambetti, G.P., Adams, J.M., Look, A.T., 2005. Slug antagonizes p53-mediated apoptosis of hematopoietic progenitors by repressing puma. Cell 123, 641–653.
Xie, Y., Zhang, K., Zhang, K., Zhang, J., Wang, L., Wang, X., Hu, X., Liang, Z., Li, J., 2020. Toll-like receptors and high mobility group box 1 in granulosa cells during bovine follicle maturation. J. Cell Physiol. 235, 3447–3462.
Yuan, J., Chen, J., 2011. The role of the human SWI5-MEI5 complex in homologous recombination repair. J. Biol. Chem. 286, 9888–9893.
Zenzes, M.T., Puy, L.A., Bielecki, R., 1997. Immunodetection of cotinine protein in granulosa-lutein cells of women exposed to cigarette smoke. Fertil. Steril. 68, 76–82.
Zenzes, M.T., Reed, T.E., 1998. Interovarian differences in levels of cotinine, a major metabolite of nicotine, in women undergoing IVF who are exposed to cigarette smoke. J. Assist Reprod. Genet 15, 99–103.
Zhou, X., He, Y., Quan, H., Yang, J., Li, S., Jiang, Y., Li, J., Yuan, X., 2024. Exposure to nicotine regulates prostaglandin E2 secretion and autophagy of granulosa cells to retard follicular maturation in mammals. Ecotoxicol. Environ. Saf. 277, 116358.